SNHG15 is involved in the progression of atherosclerosis through targeted regulation of miR-370-3p and bioinformatics analysis

Wan Pan, Yan Zhou, Fan Zhang, Yingying Zhang, Wei Li, Chengpeng Li, Liqun He*

Cardiology, Intervention Cardiology Center, Wuhan No. 1 Hospital, Wuhan, China

Submitted: 2 August 2023; **Accepted:** 9 December 2023
Online publication: 16 December 2024

Arch Med Sci
DOI: https://doi.org/10.5114/aoms/176676

***Corresponding author:**
Liqun He
Cardiology
Intervention Cardiology
Center
Wuhan No. 1 Hospital
Wuhan, China
E-mail: heliqundr@163.com

Abstract

Introduction: This study aimed to explore the expression of SNHG15 in atherosclerotic population and further evaluate the regulatory mechanism of SNHG15 in AS.
Material and methods: qRT-PCR was used to detect the level of SNHG15 in serum samples. An in vitro cell model was constructed using 50 µg/ml ox-LDL-induced VSMCs. Transwell, CCK-8 assay and ELISA were used to detect the migration, proliferation, phenotypic transformation, and inflammatory reaction of the cell model. The interaction between SNHG15 and miR-370-3p was verified by the luciferase reporter gene. Pearson analysis was used to assess the correlation between SNHG15 and miR-370-3p. The target genes of miR-370-3p and their functions were evaluated by bioinformatics analysis.
Results: The expression of SNHG15 in the AS group and ox-LDL-induced VSMCs group were upregulated ($p < 0.001$), while miR-370-3p was decreased ($p < 0.001$). *In vitro* studies showed that inhibition of SNHG15 can obviously weaken the proliferation, migration, phenotypic transformation, and inflammation of VSMCs induced by ox-LDL ($p < 0.01$). Bioinformatics and luciferase reporter gene confirmed that miR-370-3p was the downstream target gene of SNHG15. Pearson correlation coefficient revealed that miR-370-3p was negatively regulated by SNHG15 ($r = –0.6998$, $p < 0.001$). Bioinformatics analysis indicated that miR-370-3p had 160 potential target genes, whose functions were mainly related to cell cycle and cell adhesion, and were mainly concentrated in the MAPK signaling pathway. Further analysis showed that the downstream target gene of miR-370-3p was FOXO1.
Conclusions: SNHG15 mediated cell proliferation, migration, phenotypic transformation, and inflammation response via inhibiting miR-370-3p in ox-LDL-induced VSMCs.

Key words: atherosclerosis, SNHG15, miR-370-3p, vascular smooth muscle cells.

Introduction

Atherosclerosis (AS) is a major cause of cardiovascular disease, including myocardial infarction, stroke, and heart failure [1]. With the rapid growth of the global economy and the continuous improvement of human living standards, the morbidity and mortality of AS in modern society are getting higher and higher. AS usually occurs in the intima of large and medium-sized arteries, especially where blood vessels branch, which may be affected by blood flow, because the areas exposed to normal

shear stress seems to be protected [2, 3]. The main pathological features of AS are arterial lipid deposition, accompanied by proliferation of vessel smooth muscle cells (VSMCs) and fibrous matrix [4]. The formation of the atherosclerotic plaque is a sign of AS, and vascular occlusion caused by plaque rupture is an important pathophysiological mechanism for the occurrence and development of ischemic cardiovascular and cerebrovascular diseases [5]. Therefore, it is of great significance to find a mechanism that can inhibit the formation of plaque for inhibiting or alleviating the progress of AS.

In the past 30 years, with the development of high and new technologies, many new mediators or factors have been found to be involved in the pathogenesis of AS, including non-coding RNAs, intestinal flora, and immune system [6]. New generation sequencing technology reveals the long non-coding RNAs (lncRNAs) abnormalities related to the pathogenesis of AS. For example, lncRNA NEAN-AS1, which has a reduced level in human carotid atherosclerotic plaques, plays an atherosclerotic protective role by up-regulating NEXN [7]. The expression level of lncRNA smooth muscle-induced lncRNA (SMILR) in unstable plaques was higher than that in stable plaques. And it can bind to the mitotic protein centromere protein F (CENPF) mRNA, promoting smooth muscle cell proliferation [8]. LncRNA small nucleolar host gene 15 (SNHG15) is located on human chromosome 7p13, which is related to the growth of osteosarcoma, breast cancer, pancreatic cancer, and other solid cancers [9] Studies have shown increased expression of SNHG15 in patients with acute ischemic stroke [10]. Studies have also shown that inhibiting the expression of SNHG15 can significantly alleviate cerebral ischemia reperfusion injury [11]. Presently, many new studies focus on exploring the role of SNHG15 in cardiovascular disease, but its mechanism in AS is still unclear.

In recent years, competitive endogenous RNA (ceRNA), as one of the common mechanisms of miRNA, has attracted extensive attention. SNHG15 may be involved in the progress of many diseases through the mechanism of ceRNA. For example, SNHG15, as a ceRNA of miR-7, regulates the Kruppel-like factor 4 (KLF4) expression, thus delays the progression of osteoarthritis [12]. In the pathophysiology of cardiovascular disease, endothelial cells, vascular smooth muscle cells, macrophages and cardiomyocytes all contain miRNAs with different expressions. These miRNAs are powerful regulators of plaque progression and transformation into fragile states, which may eventually lead to plaque rupture, such as miR-128a and miR-499 [13]. MiR-370-3p was originally found to play a regulatory role in the development of cancer [14, 15]. Emerging evidence reveals the central role of miR-370-3p in the development of AS. Mao *et al*. reported that ox-LDL induced the decrease of miR-370-3p expression in human umbilical vein endothelial cells, and promoted apoptosis and inflammatory reaction [16]. At present, there is little research on SNHG15 as a ceRNA in the AS process.

In this study, we included patients with asymptomatic AS as a case group and those without atherosclerosis as a control group to analyze the expression of SNHG15 in these two groups and further evaluate the diagnostic value of SNHG15 in patients with asymptomatic AS. This study intends to explore the expression and function of SNHG15 and its downstream miR-370-3p in AS and further clarify the molecular mechanism of SNHG15 by using bioinformatics prediction combined with multiple biological methods such as dual luciferin reporter genes. The schematic diagram of the interaction principle of SNHG15/miR-370-3p in this study is shown in Supplementary Figure S1.

Material and methods

Recruitment of the study population

Through a retrospective study and analysis, 81 asymptomatic carotid AS patients in the hospital physical examination center were selected as the case group of this study. Inclusion criteria: 1) No history of transient cerebral ischemia or ischemic stroke before enrollment; 2) Carotid color Doppler ultrasound examination was completed to evaluate carotid intima-media thickness (CIMT). 0.9 mm ≤ CIMT < 1.2 mm is considered to be asymptomatic carotid AS [17]. Exclusion criteria: 1) Contraindications existed in imaging examination; 2) Severe cardiac, liver, and renal insufficiency; 3) Patients with brain trauma, brain tumor, cerebral hemorrhage, and history of craniocerebral surgery; 4) Patients with mental illness; 5) Patients who took anticoagulant drugs, antiplatelet drugs, or lipid-lowering drugs within 3 months before enrollment; 6) Patients with blood diseases, thyroid diseases, or malignant tumors. A total of 76 people without carotid AS who underwent physical examination at the same time in the physical examination center were selected as the control group.

All patients and their families were aware of this study and signed informed consent. This study was approved by the Ethics Committee of Wuhan No. 1 Hospital. Hospital. Blood samples of all volunteers were centrifuged to obtain the upper serum, which was stored in a –80°C refrigerator for subsequent detection.

Cell culture and grouping

VSMCs (primary aortic SMCs) were purchased from American Type Culture Collection (ATCC).

VSMCs were cultured in Dulbecco's modified eagle medium (DMEM) containing 10% Fetal bovine serum (FBS) and were incubated in a humidified incubator with 5% CO_2 at 37°C. The cell culture medium was changed every 24–48 h and cells were passaged in the ratio of 1 : 2–1 : 3. Primary VSMCs between the 3rd and 5th passages were used for further experiments. According to the published literature, the cell model of atherosclerotic injury was constructed by stimulating cells with oxidized low-density lipoprotein (ox-LDL) (Solarbio, Beijing, China). In short, ox-LDL with a concentration of 50 µg/ml was added to the cultured VSMCs, and the culture medium was changed after 12 h of incubation.

Cell transfection

VSMCs at logarithmic growth stage were selected, the cell density was adjusted to 2×10^5 cells/well and inoculated into 6-well plate. si-SNHG15 and si-NC were transfected into cells according to Lipofectamine 2000 (Invitrogen, United States) transfection kit instructions when the cells were adhered to the dish the next day and fused to 80%. After 12 h of cell transfection, the medium was replaced for follow-up experiments. The siRNA sequences were as follows: si-NC: 5'-CAGUCGCGUUUGCGACUGGC-3' (forward) and 5'-GCCAGUCGCAAACGCGACUG-3' (reverse), si-SNHG15: 5'-CCUUGAGUCUCAUGUUCAA-3' (forward) and 5'-UUGAACAUGAGACUCAAGG-3' (reverse).

Quantitative reverse transcription polymerase chain reaction (qRT-PCR)

Total RNA in serum or cells was extracted by TRIzol method. NanoDrop 2000 ultraviolet spectrophotometer was used to identify the concentration and purity of RNA. 1µg total RNA was used as template for reverse transcription, and then cDNA was used as template for qRT-PCR. The reaction system consisted of cDNA 1 µl, 2× SYBR Green Premix (Takara, Japan) 10 µl, forward primer 1 µl, reverse primer 1 µl, and finally RNA-free water was added to 20 µl. The reaction conditions were pre-denaturation at 95°C for 5 min, followed by 40 cycles of denaturation at 95°C for 30 s, annealing at 58°C for 30 s and extension at 70°C for 30 s. The internal reference gene was GAPDH and the results were analyzed by $2^{-\Delta\Delta Ct}$ method. The primers used in this study were as follows: SNHG15 forward primer: 5'-CTGAGGTGACGGTCTCA-3', SNHG15 reverse primer: 5'-GCCTCCCAGTTTCATGG-3'. GAPDH forward primer: 5'-AGCCACATCGCTCAGACA-3', GAPDH reverse primer: 5'-TGGACTCCACGACGTACT-3'.

Cell migration

Cell migration ability was evaluated by Transwell method. The brief procedure was as follows: the cells were grouped according to the experimental procedure. After 24 h of cell culture, cells from each group were collected using serum-free medium, and cell density was adjusted to 5×10^4 cells/ml. Subsequently, 200 µl cell suspension was added to the upper chamber of Transwell, and 500 µl complete medium was added to the lower chamber. After 24 h of cell culture, cells were fixed with 4% paraformaldehyde for 30 min, stained with 0.4% crystal violet for 15 min, and finally observed and counted by the inverted microscope.

Cell viability

Cell viability was detected by the cell counting kit-8 (CCK-8) assay. The transfected cells were inoculated into 96-well plates according to the density of 8000 cells/well. Each group was provided with 3 multiple wells, and the cell-free wells were used as blank control. Ox-LDL was stimulated after the cells were attached to the cell dish. The culture medium was replaced, and the culture plate was placed in the incubator. The culture plate was removed at the predetermined time point (0 h, 24 h, 48 h, 72 h) and 10 µl CCK-8 solution was added to each well for continued incubation for 4 h. Finally, OD value at 450 nm was measured by the microplate reader (Bio-Rad, United States) and cell viability was calculated.

Enzyme-linked immunosorbent assay (ELISA)

The cell supernatant of each group after treatment was collected according to the experimental requirements. The contents of inflammatory cytokines such as interleukin-1β (IL-1β), IL-6, tumor necrosis factor-α (TNF-α) and phenotypic transformation markers of VSMCs (α-smooth muscle actin, α-SMA; osteopontin (OPN)) were determined using a commercially available ELISA kit (R&D Systems, Minneapolis, MN, USA), and the specific experimental procedures were carried out in strict accordance with the instructions of the kit.

Luciferase reporter gene assay

Online target gene software prediction showed that SNHG15 had binding sites with miR-370-3p. The 3'-UTR sequence of SNHG15 was obtained from the gene bank, and GenePharma (Shanghai, China) was commissioned to synthesize the 3'-UTR wild-type nucleotide sequence of SNHG15 including the binding site of miR-370-3p, while the mutant sequence of the 3'-UTR wild-type sequence of SNHG15 was mutated at the binding site of miR-370-3p. The amplified product was inserted into the SacI and XhoI restriction sites of a pmirGLO vector to produce a wild-type and mutant pmirGLO dual luciferase reporter vector. The logarithmic growth stage VSMCs were inoc-

ulated into 6-well plates (1×10^5 cells/well), and cultured for 24 h, then the serum-free medium was replaced. SNHG15-WT or SNHG15-MUT vectors and miR-370-3p mimic/inhibitor or inhibitor/mimic-NC were co-transfected into cells using Lipofectamine 2000 kit. After 24 h of cell culture, the cells were collected, and the supernatant was taken after the cells were fully lysed. The activities of Renilla and firefly luciferase were detected by the dual-luciferase reporting system, with Renilla luciferase as the internal reference.

Prediction of miR-370-3p target genes and bioinformatics analysis

TargetScan 8.0, miRDB and EVmiRNA databases were used to predict the target genes of miR-370-3p, and Venn diagram were drawn. Gene Ontology (GO) analysis of the previously predicted miR-370-3p target genes was performed using the DAVID 6.8 database to determine the molecular functions (MF), biological processes (BP), and cellular components (CC) of these target genes. Kyoto Encyclopedia of Genes and Genomes (KEGG) database was used to analyze the possible enrichment signal pathways of target genes. Subsequently, a protein-protein interaction (PPI) network was established using STRING v11.0 database to study the interaction between these target genes.

Statistical analysis

SPSS 17.0 and GraphPad Prism 8.0 were used for statistical analysis and image rendering. Measurement data were expressed as mean ± standard deviation. Two or more groups were compared using independent sample t test and one-way analysis of variance (ANOVA). Receiver operator characteristic (ROC) curve was used to study the diagnostic significance of serum SNHG15 in AS population. Pearson correlation coefficient was used to analyze the correlation between SNHG15 and carotid intima media thickness (CIMT). All cell experiments were performed with $n = 5$ samples per group. $P < 0.05$ was considered as significant difference.

Results

Comparison of baseline data and clinical characteristics

The clinical data of the control group and the AS group are summarized in Table I. The two groups of volunteers were matched in gender, age, and body mass index (BMI) and were comparable ($p > 0.05$). The results showed that the values of total cholesterol (TC), low-density lipoprotein cholesterol (LDL-C), fasting blood glucose (FBG), systolic blood pressure (SBP), diastolic blood pressure (DBP) and CIMT in the AS group were significantly higher than those in the control group ($p < 0.05$). There were no significant differences in triglyceride (TG), high-density lipoprotein cholesterol (HDL-C) and other indexes between the two groups ($p > 0.05$). Besides, in the AS group, there were 48 cases of hypertension, 72 cases of hyperlipidemia and 7 cases of diabetes.

Correlation between SNHG15 and clinical indicators in patients with AS

The analysis results of Pearson correlation coefficient are shown in Table II. The results showed

Table I. Baseline data and characteristics of all subjects

Characteristics	Control ($n = 76$)	Atherosclerosis ($n = 81$)	P-value
Gender (males/females)	43/33	45/36	0.513
Age [years]	57.36 ±5.45	56.86 ±6.07	0.162
BMI [kg/m^2]	24.43 ±2.18	24.77 ±2.86	0.980
TC [mmol/l]	4.02 ±1.03	5.42 ±1.07	< 0.001
TG [mmol/l]	1.39 ±0.68	1.43 ±0.79	0.466
LDL-C [mmol/l]	3.03 ±0.68	3.75 ±0.96	0.002
HDL-C [mmol/l]	1.83 ±0.56	1.69 ±0.74	0.266
FBG [mmol/l]	4.67 ±0.81	5.13 ±1.02	0.025
SBP [mm Hg]	125.53 ±11.04	151.36 ±15.19	< 0.001
DBP [mm Hg]	78.8 5±9.58	84.94 ±10.07	< 0.001
CIMT [mm]	0.64 ±0.15	1.24 ±0.17	< 0.001
Hypertension n (%)	/	48 (59.3%)	/
Hyperlipidemia n (%)	/	72 (88.9%)	/
DM n (%)	/	1 (1.2%)	/

BMI – body mass index, TC – total cholesterol, TG – triglyceride, LDL-C – low-density lipoprotein cholesterol, HDL-C – high-density lipoprotein cholesterol, FBG – fasting blood-glucose, SBP – systolic blood pressure, DBP – diastolic blood pressure, CIMT – carotid intima-media thickness, DM – diabetes mellitus. Data are expressed as n or mean ± standard deviation (SD).

Table II. Correlation analysis between SNHG15 and various indicators

Characteristics	Bivariate correlation		Multiple linear regression			
	r	*P*-value	Coefficient	Standard error	*r*	*P*-value
TC [mmol/l]	0.632	< 0.001	0.082	0.032	2.516	0.014
LDL-C [mmol/l]	0.588	< 0.001	0.025	0.030	0.837	0.405
SBP [mm Hg]	0.591	< 0.001	0.001	0.001	0.871	0.386
DBP [mm Hg]	0.618	< 0.001	0.006	0.003	2.033	0.041
CIMT [mm]	0.680	< 0.001	0.018	0.009	6.132	< 0.001

TC – total cholesterol, LDL-C – low-density lipoprotein cholesterol, SBP – systolic blood pressure, DBP – diastolic blood pressure, CIMT – carotid intima-media thickness.

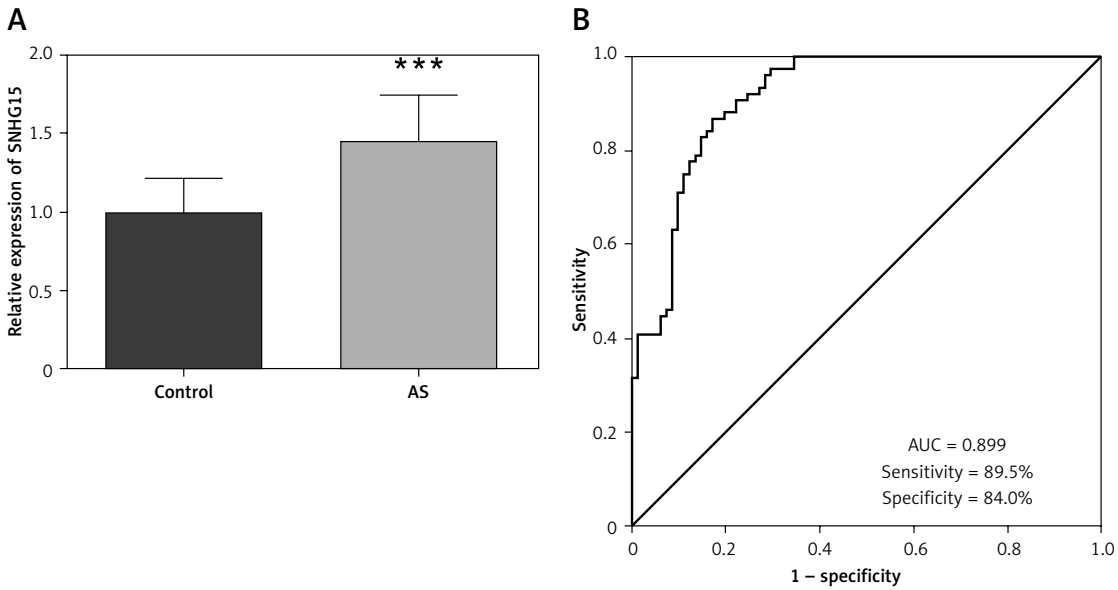

Figure 1. Expression and clinical diagnostic value of long non-coding RNA SNHG15 in asymptomatic patients with carotid atherosclerosis. **A** – PCR results showed that SNHG15 expression was increased in the atherosclerosis (AS) group. **B** – The receiver operator characteristic (ROC) curve showed that the area under the curve (AUC) of SNHG15 was 0.899, the sensitivity and specificity were 89.5% and 84.0%, respectively. $^{***}P < 0.001$ vs. the control group

that the levels of TC ($r = 0.632$, $p < 0.001$), LDL-C ($r = 0.588$, $p < 0.001$), SBP ($r = 0.591$, $p < 0.001$), DBP ($r = 0.618$, $p < 0.001$) and CIMT ($r = 0.680$, $p < 0.001$) were significantly positively correlated with the levels of SNHG15.

SNGH15 was enhanced in asymptomatic atherosclerosis patients and showed positive significance in differentiating asymptomatic AS

The expression of SNHG15 in serum was detected by qRT-PCR. Compared with the control group, the expression trend of SNHG15 was detected to be increased in the AS group (Figure 1 A, $p < 0.001$). Further, ROC curve analysis was performed for the relative expression level of serum SNHG15 in all subjects. The results presented in Figure 1 B showed that the area under the curve (AUC) of SNHG15 was 0.899, and the sensitivity and specificity of the curve were 89.5% and 84.0%, respectively, indicating that SNHG15 had high diagnostic accuracy in distinguishing AS from the control group.

Inhibition of SNHG15 is helpful in alleviating abnormal migration, proliferation, phenotypic transformation, and inflammation of ox-LDL-induced VSMCs

An *in vitro* atherosclerosis cell model was constructed by ox-LDL-induced VSMCs. The results showed that SNHG15 expression was enhanced in ox-LDL-induced VSMCs. However, the *in vitro* cell transfection technique can reduce the expression level of SNHG15 by transfecting si-SNHG15 cells (Figure 2 A, $p < 0.001$). Moreover, cell migration and proliferation experiments showed that the migration and proliferation of VSMCs were enhanced after ox-LDL treatment. In this case, downregulation of SNHG15 could significantly inhibit the abnormal migration and proliferation of VSMCs (Figures 2 B–D, $p < 0.001$). For phenotypic transformation of VSMCs, downregulation of SNHG15 significantly increased the level of the systolic marker α-SMA while decreasing the expression of the synthetic marker OPN (Figure 2 E,

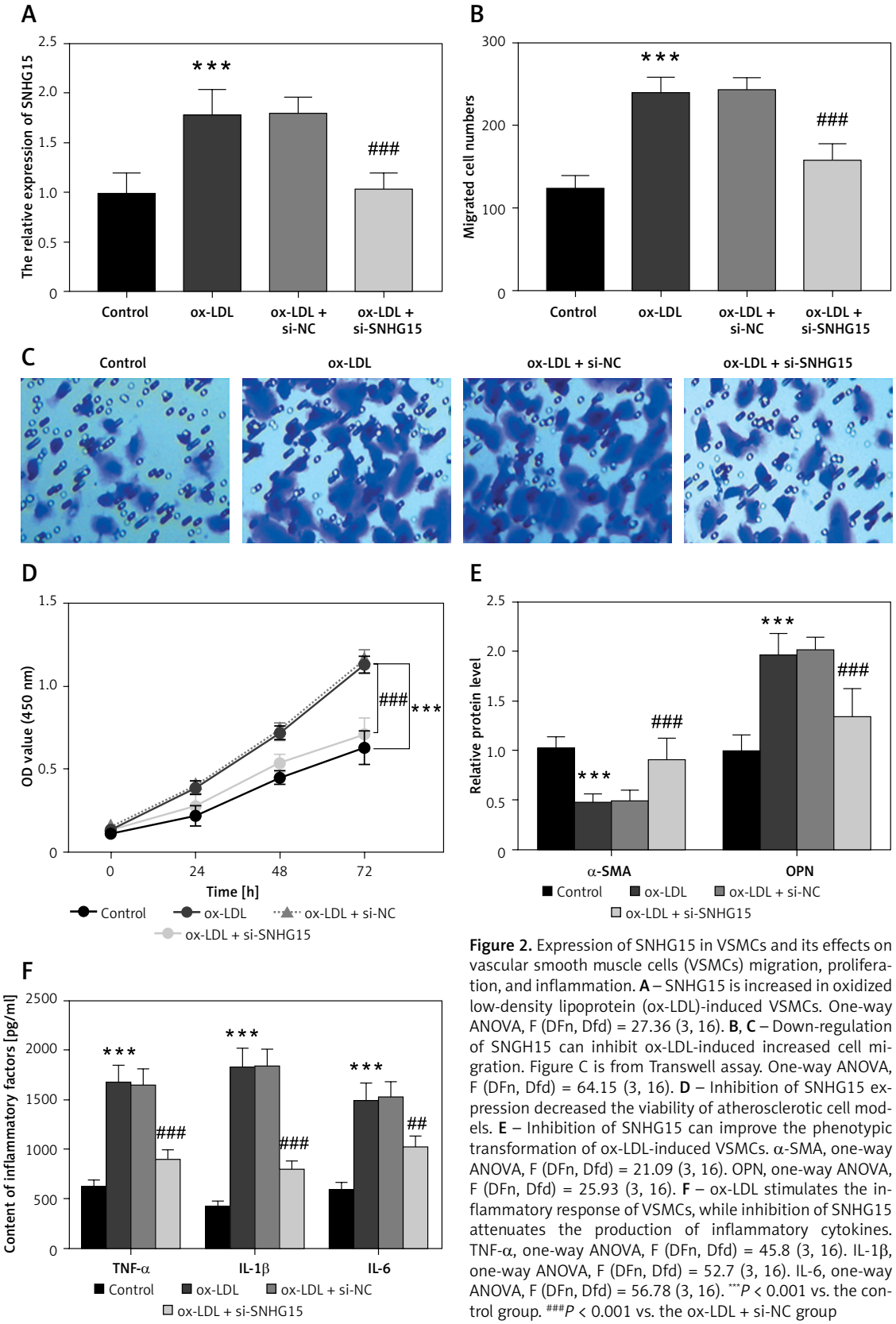

Figure 2. Expression of SNHG15 in VSMCs and its effects on vascular smooth muscle cells (VSMCs) migration, proliferation, and inflammation. **A** – SNHG15 is increased in oxidized low-density lipoprotein (ox-LDL)-induced VSMCs. One-way ANOVA, F (DFn, Dfd) = 27.36 (3, 16). **B**, **C** – Down-regulation of SNGH15 can inhibit ox-LDL-induced increased cell migration. Figure C is from Transwell assay. One-way ANOVA, F (DFn, Dfd) = 64.15 (3, 16). **D** – Inhibition of SNHG15 expression decreased the viability of atherosclerotic cell models. **E** – Inhibition of SNHG15 can improve the phenotypic transformation of ox-LDL-induced VSMCs. α-SMA, one-way ANOVA, F (DFn, Dfd) = 21.09 (3, 16). OPN, one-way ANOVA, F (DFn, Dfd) = 25.93 (3, 16). **F** – ox-LDL stimulates the inflammatory response of VSMCs, while inhibition of SNHG15 attenuates the production of inflammatory cytokines. TNF-α, one-way ANOVA, F (DFn, Dfd) = 45.8 (3, 16). IL-1β, one-way ANOVA, F (DFn, Dfd) = 52.7 (3, 16). IL-6, one-way ANOVA, F (DFn, Dfd) = 56.78 (3, 16). $^{***}P < 0.001$ vs. the control group. $^{###}P < 0.001$ vs. the ox-LDL + si-NC group

$p < 0.001$). For inflammatory response, inhibition of SNHG15 clearly suppressed the production of ox-LDL-induced intracellular inflammatory cytokines such as TNF-α, IL-1β and IL-6 (Figure 2 F, $p < 0.001$). The transfection efficiency of SNHG15 and the effect of down-regulation of SNHG15 on control cells are shown in Supplementary Figure S2.

SNHG15 adsorbs miR-370-3p and targets to negatively regulate the expression of miR-370-3p

Starbase V2.0 online database predicts many miRNAs targeted by SNHG15, including miR-370-3p (Supplementary Table SI for detailed data). The complementary sites of SNHG15 and miR370-3p are shown in Figure 3 A. Dual luciferase assay results showed that compared with the control group, the relative luciferase activity of WT-SNHG15 was significantly decreased or increased after transfection with miR-370-3p mimic or miR-370-3p inhibitor (Figure 3 B, $p < 0.001$). There was no significant change in luciferase activity in the group containing MUT-SNHG15 (Figure 3 B, $p > 0.05$). The results presented in Figure 3 C showed that compared with the control group, the content of miR-370-3p in the serum of AS patients was significantly reduced ($p < 0.001$). Pearson correlation analysis showed that the expression level of miR-370-3p in the AS group was negatively correlated with the expression level of SNHG15, and was

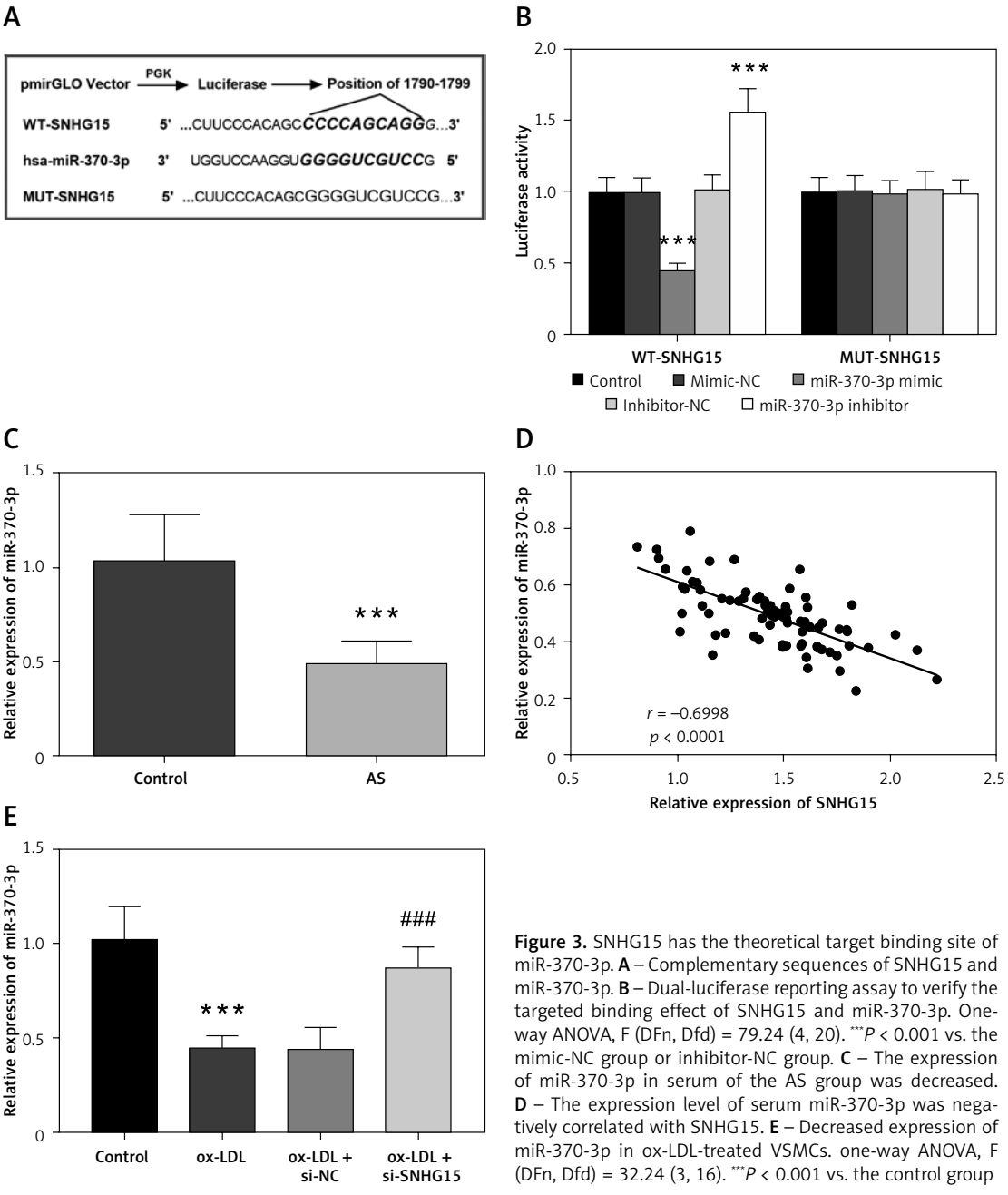

Figure 3. SNHG15 has the theoretical target binding site of miR-370-3p. **A** – Complementary sequences of SNHG15 and miR-370-3p. **B** – Dual-luciferase reporting assay to verify the targeted binding effect of SNHG15 and miR-370-3p. One-way ANOVA, F (DFn, Dfd) = 79.24 (4, 20). $^{***}P < 0.001$ vs. the mimic-NC group or inhibitor-NC group. **C** – The expression of miR-370-3p in serum of the AS group was decreased. **D** – The expression level of serum miR-370-3p was negatively correlated with SNHG15. **E** – Decreased expression of miR-370-3p in ox-LDL-treated VSMCs. one-way ANOVA, F (DFn, Dfd) = 32.24 (3, 16). $^{***}P < 0.001$ vs. the control group

negatively regulated by SNHG15 (Figure 3 D, $r = -0.6998$, $p < 0.001$). In addition, *in vitro* cell experiments showed that miR-370-3p was decreased in ox-LDL-induced VSMCs, while down-regulating the expression of SNHG15 aggrandized the content of miR-370-3p, which further confirmed the relationship between SNHG15 and miR-370-3p (Figure 3 E, $p < 0.001$).

Inhibition of miR-370-3p negates the positive effect of silencing SNHG15 on ox-LDL-induced VSMCs

In order to further verify the effect of miR-370-3p on VSMCs, cell transfection technology was used to regulate the expression of miR-370-3p. The results showed that transfection with miR-370-3p inhibitor significantly attenuated the increase of miR-370-3p caused by the reduction of SNHG15 (Figure 4 A, $p < 0.001$). Transwell and CCK-8 assays showed that downregulating SNHG15 could inhibit the abnormal migration and proliferation of VSMCs, while the above effects were overturned after the inhibition of miR-370-3p (Figures 4 B–D, $p < 0.001$). As shown in Figure 4 E, the reduction of miR-370-3p overturns the inhibition of phenotypic transformation due to SNHG15 suppression and produces an ox-LDL-like effect, characterized by a decrease in systolic markers and an increase in synthetic markers ($p < 0.01$). Figure 4 F showed that inhibiting the expression of SNHG15 can reduce the production of inflammatory factors, while simultaneously down-regulating miR-370-3p can aggravate the inflammatory response ($p < 0.01$).

Bioinformatics analysis of miR-370-3p

Three databases, including TargetScan 8.0, miRDB and EVmiRNA, were used to predict the target genes of miR-370-3p, and the Venn diagram was constructed. As shown in Figure 5 A, the number of target genes supported by the three databases is 160. The names of these 160 target genes are shown in Table III for subsequent analysis.

The GO enrichment analysis of 160 possible target genes of miR-370-3p is shown in Figure 5 B. The results showed that these 160 target genes were mainly distributed in the early endosomes and were mainly involved in regulating the activity of protein serine/threonine kinases, ion binding, transcription factor binding and other molecular functions ($p < 0.05$). In addition, these 160 target genes are involved in a variety of biological processes, including cell cycle, mitosis, cell adhesion, neuronal apoptosis ($p < 0.05$). Further, the KEGG pathway analysis results showed that the mechanism of the target genes mainly focused on the regulation of mitogen-activated protein kinases (MAPK) signaling pathway, insulin signaling pathway, mammalian target of rapamycin (mTOR) signaling pathway and hypoxia-inducible factor (HIF-1) signaling pathway (Figure 5 C, $p < 0.05$).

We performed a PPI network analysis in order to better understand the pathogenesis of atherosclerosis. First, PPI networks of miR-370-3p target genes were constructed. During the STRING database test, the minimum interaction score required was set to 0.500. The PPI network has a total of 474 interactions (connections) and 159 nodes (Figure 6). According to the nature of the network topology, there are 53 key nodes with a degree value and above the average value (degree value = 1.48). This represents 33.33% of the total number of nodes. Table IV listed the top ten target genes according to the ranking of degrees.

FOXO1 is the downstream target gene of miR-370-3p in VSMCs

The complementary sequences and loci of miR-370-3p and FOXO1 are shown in Figure 7 A. As shown in Figure 7 B, the luciferase reporter gene showed that the luciferase activity of the WT-FOXO1 group was decreased or increased with the transfection of miR-370-3p mimic and miR-370-3p inhibitor ($p < 0.001$), but this phenomenon was not observed in the MUT group. In the serum samples of the subjects, FOXO1 expression was up-regulated compared with that of the control group (Figure 7 C, $p < 0.001$). In addition, cell studies showed increased FOXO1 expression in ox-LDL-induced cell models, consistent with results in clinical samples. Subsequent inhibition of SNHG15 significantly down-regulated FOXO1 expression. Further, the expression of FOXO1 increased after the inhibition of miR-370-3p (Figure 7 D, $p < 0.001$).

Discussion

AS is a disease of narrowing of arteries due to plaque accumulation. VSMCs are involved in the progression of AS [18]. Our study aims to evaluate the role of SNHG15 in AS and its possible mechanisms. The results showed that the expression of SNHG15 was increased in asymptomatic AS patients, and it had certain clinical diagnostic value. In addition, cell studies showed that highly expressed SNHG15 promoted the proliferation, migration, apoptosis and phenotypic transformation of the AS inflammatory model by inhibiting miR-370-3p, and accelerated the damage of the AS cell model.

Presently, a large number of studies have shown that lncRNAs are closely related to the development of cardiovascular diseases. They participate in heart remodeling, heart failure and

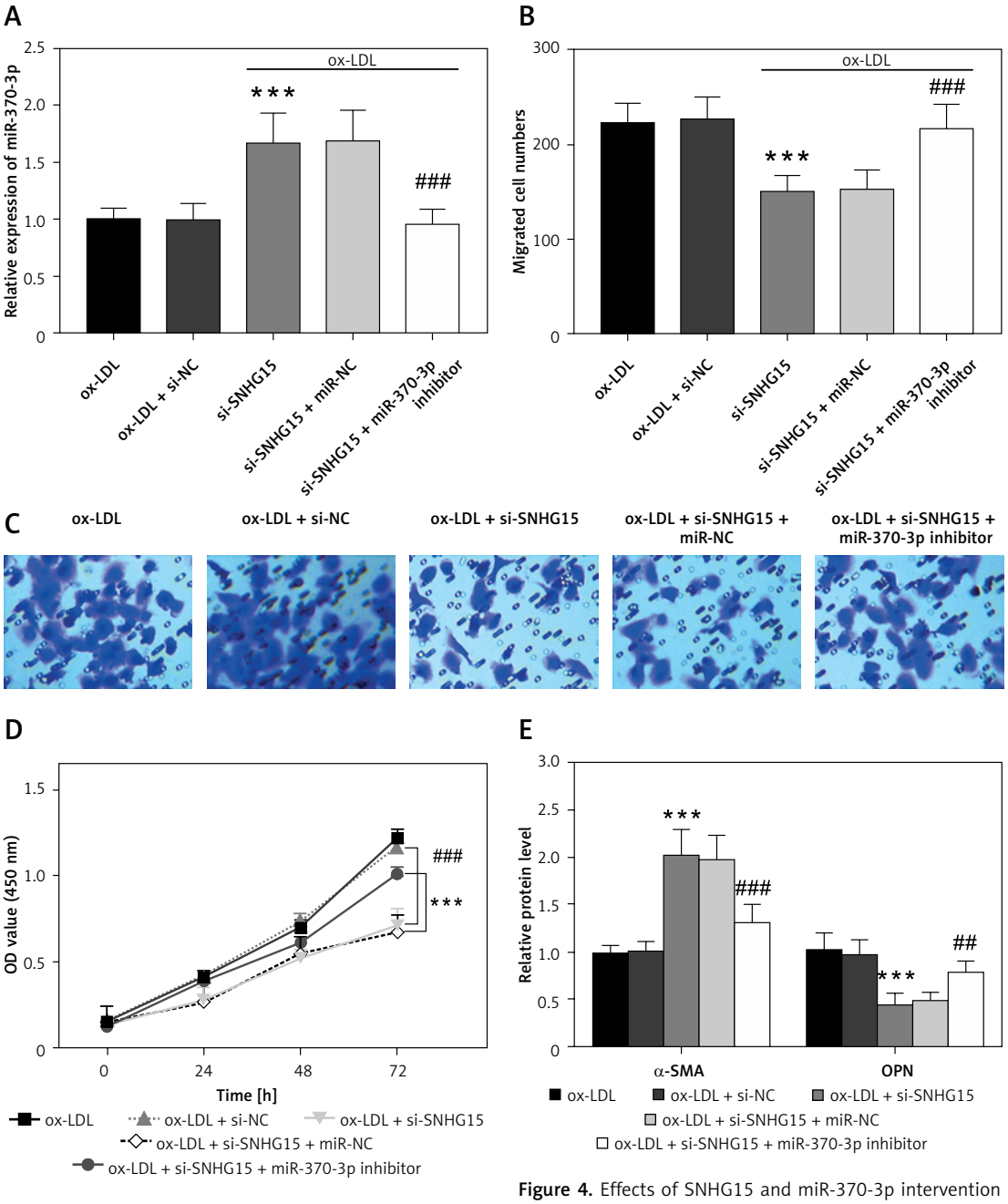

Figure 4. Effects of SNHG15 and miR-370-3p intervention on ox-LDL-induced VSMCs migration, proliferation, and inflammation. **A** – The presence of miR-370-3p inhibitors down-regulates the increased expression of miR-370-3p due to the inhibition of SNHG15. One-way ANOVA, F (DFn, Dfd) = 20.44 (4, 20). **B**, **C** – The decrease of miR-370-3p promotes the enhancement of cell migration. Figure C is from Transwell assay. One-way ANOVA, F (DFn, Dfd) = 18.34 (4, 20). **D** – Inhibition of miR-370-3p enhanced the cell viability of VSMCs. **E** – The reduction of miR-370-3p reversed the inhibitory effect of silencing SNHG15 on phenotypic transformation of VSMCs. α-SMA, one-way ANOVA, F (DFn, Dfd) = 84.06 (4, 20). OPN, one-way ANOVA, F (DFn, Dfd) = 11.3 (4, 20). **F** – Inhibition of miR-370-3p reverses the inflammatory inhibition caused by downregulation of SNHG15. TNF-α, one-way ANOVA, F (DFn, Dfd) = 22.68 (4, 20). IL-1β, one-way ANOVA, F (DFn, Dfd) = 31.54 (4, 20). IL-6, one-way ANOVA, F (DFn, Dfd) = 29.07 (4, 20). $^{**}P < 0.01$, $^{***}P < 0.001$ vs. the ox-LDL + si-NC group. $^{\#\#}P < 0.01$, $^{\#\#\#}P < 0.001$ vs. the ox-LDL + si-SNHG15 + miR-370-3p inhibitor group

Table III. The 160 target genes of miR-370-3p predicted by TargetScan, miRDB and EVmiRNA databases

AFF1	CA12	DOCK4	HMGA2	LRTM2	PEAK1	SLC4A4
AKAP10	CANX	DRD5	HMGXB3	MAML1	PIK3CA	SMO
ALAD	CASK	DSTYK	HSP90AB1	MAP2K7	POFUT1	SNRNP25
ANK3	CASQ2	ECE1	HSPBAP1	MATR3	PRKACB	SORT1
APOL3	CCDC170	EGLN3	IGF2BP1	MBNL1	PRPF38A	SRSF6
AQP4	CCNE2	EIF2B1	IL16	MCFD2	PRRX1	SZT2
AR	CCNJ	EXOC7	IL18BP	MGMT	RAB15	TENM2
ARID3B	CD40	FAM3A	IL5RA	MKNK1	RAB7A	TGFBR2
ARSD	CDC25B	FBLN5	ILF3	MLC1	RAD54L2	TMEM127
ASCC1	CHD2	FCGR3A	ING3	MR1	RASSF1	TMEM231
ATPAF2	CHST11	FCGR3B	INO80	MYF6	RBPJ	TNRC6B
ATRN	CIT	FGF7	KAT6A	NDST1	RETSAT	TNS1
ATXN1	CLIC6	FOXO1	KCNJ11	NF1	RUNX1T1	TPM4
AURKA	CNTNAP1	FOXO4	KCNK3	NFASC	SCG3	TPO
BAG4	COL26A1	FRAS1	KCNQ4	NR4A3	SGCD	TRIB2
BAP1	CRLF1	FRMD4B	KCTD15	ODF2	SH3BP2	UBTF
BBS12	CRYAA	GABBR2	KDR	ORC5	SH3D19	UPF2
BCL2L11	CYB561D1	GPD1	KIAA0355	PACS1	SH3PXD2A	WNT10B
BEX2	CYP2U1	GRB10	KLHL3	PARVB	SIX1	WNT9B
BHLHB9	DCK	GRIK3	KRT80	PAX5	SLC10A7	XYLT1
BICD2	DDX3X	GSS	LAMC3	PBX1	SLC16A2	ZDHHC15
BRF1	DHX33	HDAC4	LDLRAP1	PDE7A	SLC25A24	ZFP90
C2	DNAJB1	HDX	LIN28A	PDHB	SLC46A1	

other disease processes by regulating cell differentiation, proliferation, and apoptosis [19]. These lncRNAs can be used not only as biomarkers, but also as potential targets for disease treatment or important indicators for predicting prognosis. For example, lncRNA SENCR alleviates TGF-β-induced endothelial-to-mesenchymal transition by directly inhibiting TGF-β/Smad signaling pathway, thereby alleviating atherosclerosis progression [20]. As shown in this study, compared with non-AS populations, SNHG15 was found to be significantly elevated in patients with AS, suggested that dysregulation of SNHG15 may play a role in the development of AS. Further, from ROC analysis, it can be seen that SNHG15; shows high clinical diagnosis accuracy in distinguishing asymptomatic AS from healthy people, and also shows the clinical diagnostic value of SNHG15 for asymptomatic AS. An in vitro atherosclerotic cell model was established by inducing VSMCs with ox-LDL. VSMCs are the main source of collagen in the fibrous cap of the plaque, which is beneficial and necessary for plaque stability [21]. Under the influence of AS pathogenic factors, VSMCs were damaged and secrete a lot of inflammatory factors. Subsequently, due to inflammation and oxidative stress, the mesothelial VSMCs changed from the mature contraction phenotype to the synthetic type, which enhanced the proliferation and migration ability of VSMCs, increased their sensitivity and disappeared their contraction function [22, 23]. In this study, the expression of SNHG15 was up-regulated after ox-LDL treatment. ox-LDL treatment triggered the inflammatory reaction and enhanced the proliferation and migration ability of VSMCs. At the same time, it was also observed that ox-LDL treatment intensified the phenotypic transformation of VSMCs from the contraction phenotype to the secretory phenotype, which was manifested by the decrease of α-SMA and the increase of OPN. It is worth noting that the adverse effects of ox-LDL on VSMCs can be alleviated after down-regulating SNHG15.

In order to further explore the mechanism of SNHG15 in AS, we confirmed that miR-370-3p was the target gene of SNHG15 through the bioinformatics analysis and Luciferase report gene assay. The research on the targeting relationship between SNHG15 and miR-370-3p has been discovered by Wang *et al.* in the study of ovarian can-

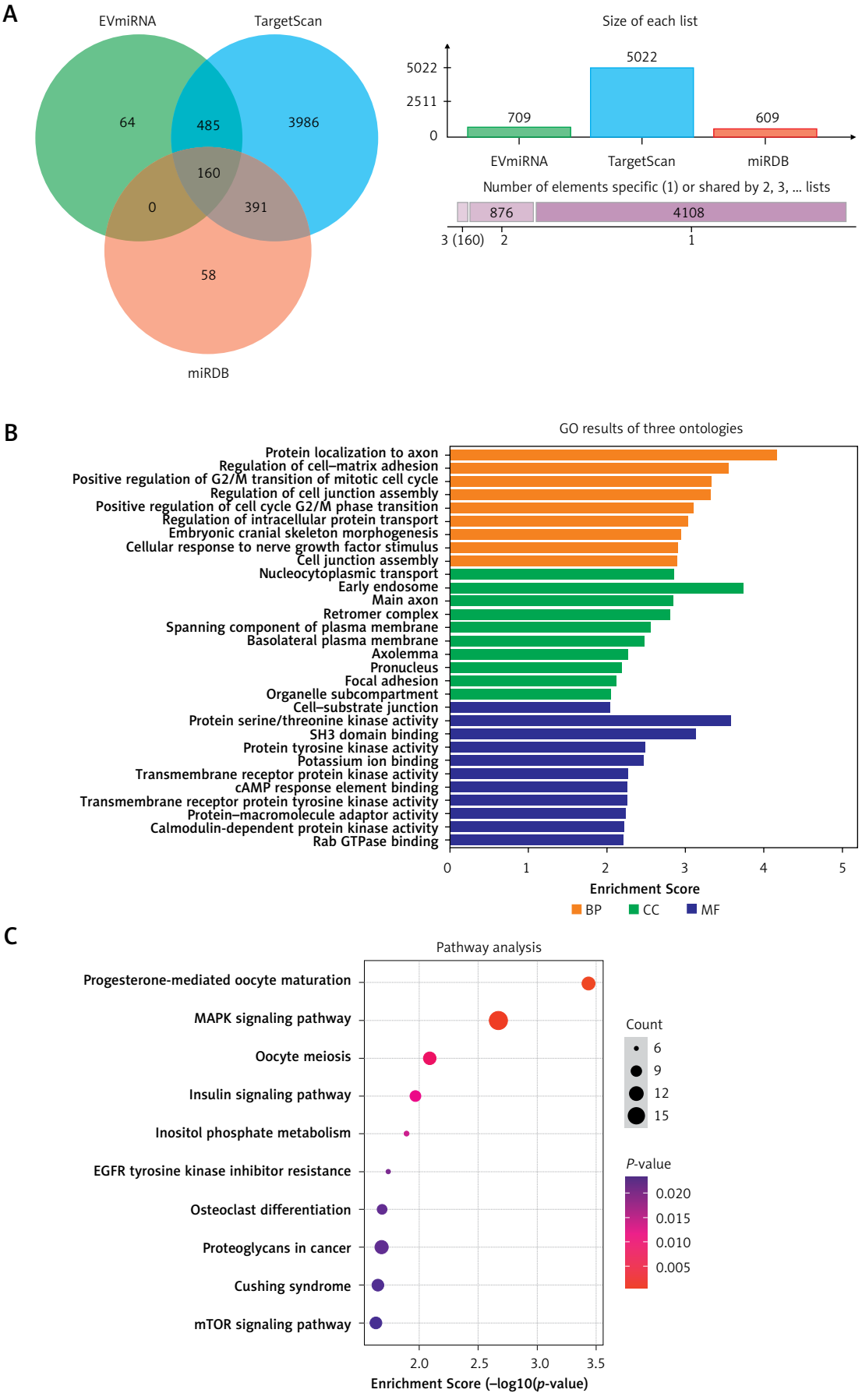

Figure 5. Bioinformatics analysis of miR-370-3p. **A** – Venn diagram of miR-370-3p target gene prediction. **B** – GO enrichment analysis of the miR-370-3p target gene. **C –** KEGG pathway analysis of the miR-370-3p target gene

BP – biological process, CC – cellular component, MF – molecular function.

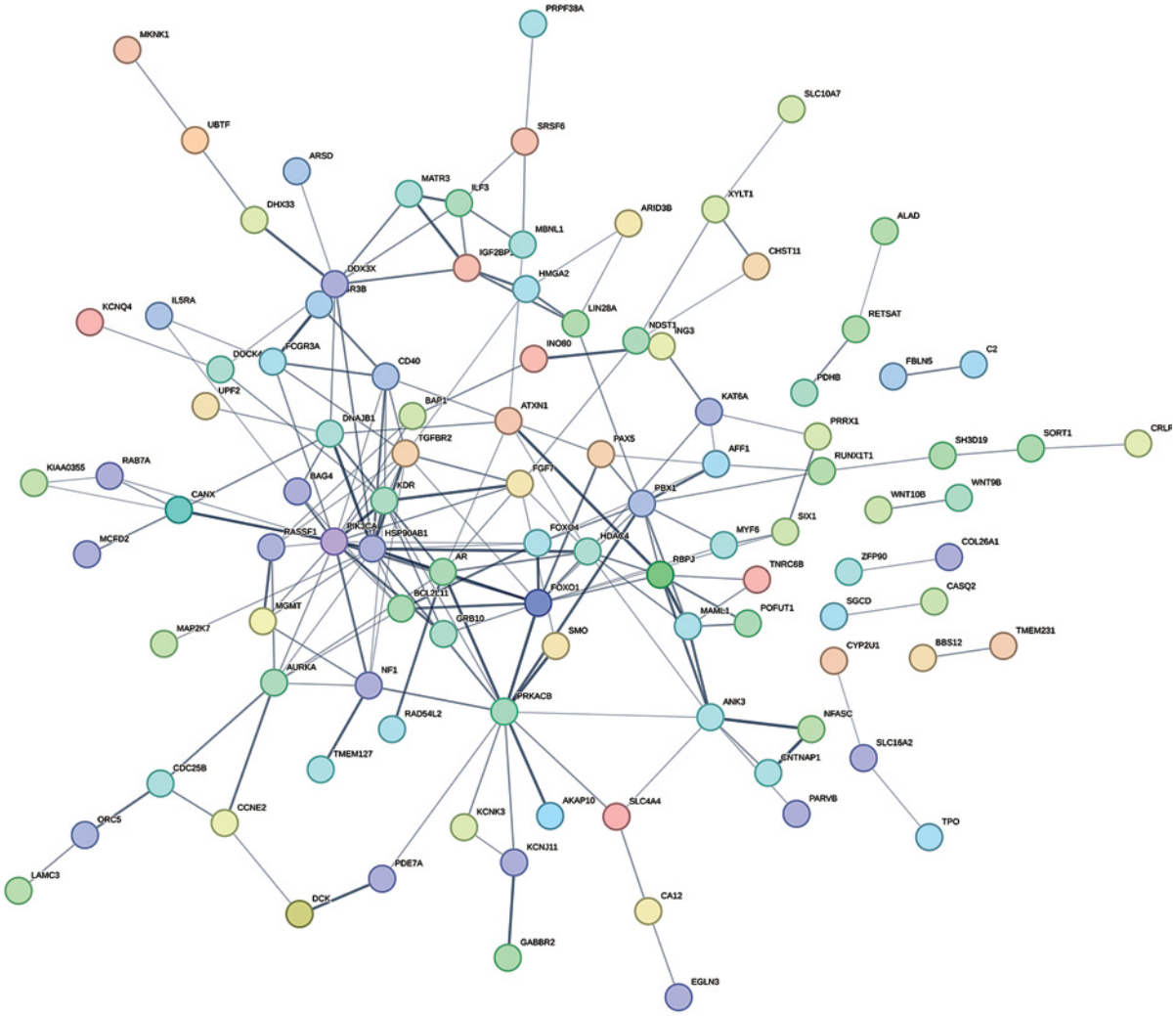

Figure 6. STRING protein-protein interaction network of the 160 mRNAs

Table IV. Topology characteristics of hub nodes in the PPI network

No.	Node	Description	Degree
1	PIK3CA	Phosphatidylinositol 4,5-bisphosphate 3-kinase catalytic subunit alpha isoform	19
2	HSP90AB1	Heat shock protein HSP 90-beta	16
3	PRKACB	cAMP-dependent protein kinase catalytic subunit beta	9
4	FOXO1	Forkhead box protein O1	7
5	PBX1	Pre-B-cell leukemia transcription factor 1	7
6	RBPJ	Recombining binding protein suppressor of hairless	5
7	AR	Androgen receptor	5
8	KDR	Vascular endothelial growth factor receptor 2	5
9	DDX3X	ATP-dependent RNA helicase DDX3X	4
10	DNAJB1	DnaJ homolog subfamily B member 1	4

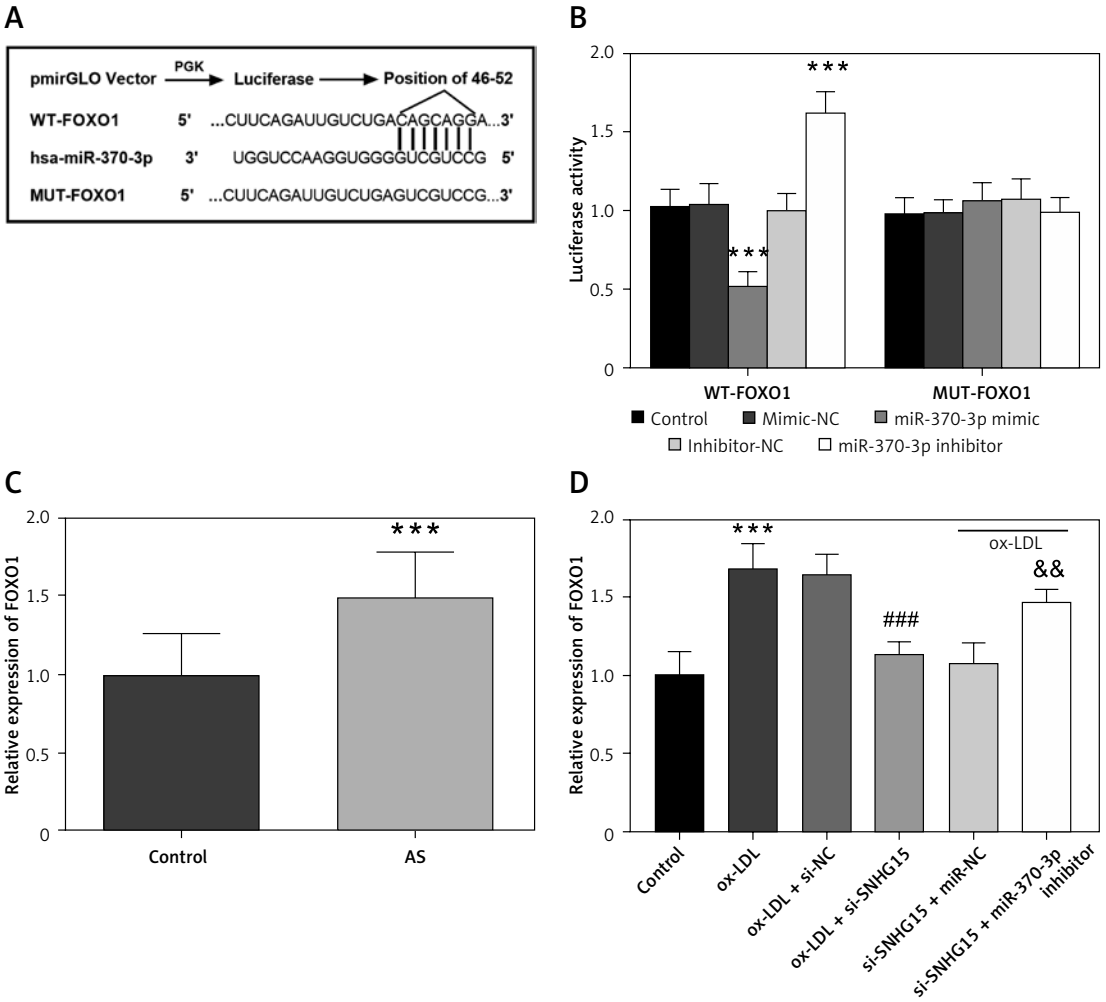

Figure 7. FOXO1 is a downstream target gene of miR-370-3p. **A** – Complementary sequence of miR-370-3p and FOXO1. **B** – Dual-luciferase reporting assay to verify the targeted binding effect of miR-370-3p and FOXO1. One-way ANOVA, F (DFn, Dfd) = 69.87 (4, 20). $^{***}P < 0.001$ vs. the mimic-NC group or inhibitor-NC group. **C** – The expression of FOXO1 in serum of the AS group was detected using qRT-PCR. **D –** Increased expression of FOXO1 in ox-LDL-treated VSMCs. One-way ANOVA, F (DFn, Dfd) = 30.51 (5, 24). $^{***}P < 0.001$ vs. the control group

cer [24]. miR-370-3p has been proved to be abnormally expressed in cardiovascular disease. Ding *et al.*'s research showed that the inhibition of miR-370-3p reversed the inhibition of VMSC viability and migration mediated by circ-0010283 silencing [25]. An animal experiment showed that the overexpression of miR-370-3p could significantly inhibit fat accumulation. On the contrary, the decrease of miR-370-3p inhibited the proliferation of 3T3-L1 preadipocytes and promoted the differentiation of preadipocytes [26]. A recent study by Hildebrandt *et al.* revealed abnormal expression of miRNAs in AS-related complications, in which the expression of miR-370-3p in blood of patients with coronary heart disease was significantly reduced [27]. All the above studies directly or indirectly illustrate that miR-370-3p plays an important regulatory role in AS. In this study, we found that the inhibition of miR-370-3p destroyed the restrictive effect of silencing SNHG15 on the proliferation, migration, and inflammation of VSMCs. This result was consistent with many of the above research, which further explained the relationship between SNHG15 and miR-370-3p on VSMCs.

The essence of miRNA in disease regulation is to regulate target genes in disease-related signaling pathways. This study and several previously published papers have confirmed that miR-370-3p is involved in the occurrence and development of AS, but the specific regulatory target gene network is still unclear. Bioinformatics analysis is an important means to predict the target genes of miRNA, and the potential target genes of miRNA can be identified through bioinformatics technology, which provides ideas and directions for subsequent verification of their functions. In this study, three databases were used to predict the target genes of miR-370-3p, namely TargetScan, miRDB and EVmiRNA, and 160 potential target genes were obtained from the intersection of the three databases. In order to

further clarify the function of these potential target genes, GO and KEGG enrichment analysis was performed in this study. GO analysis showed that these target genes were mainly involved in various biological processes such as cell cycle, mitosis, and cell adhesion. KEGG analysis showed that these target genes were mainly concentrated in the MAPK signaling pathway, mTOR signaling pathway, HIF-1 signaling pathway and insulin signaling pathway. It has been confirmed that vascular damage and inflammation caused by various factors including hypertension and hyperglycemia can induce local VSMC to undergo the cell cycle and over-proliferation in the subintima [28]. The abnormal cell cycle plays a key role in the pathological development of AS and a series of pathological processes of coronary restenosis in AS. The impaired vascular endothelial function is the initial stage of AS. Studies have shown that lipids activate nuclear factor-κB (NF-κB) through the MAPK signaling pathway, promote endothelial cells to secrete a large number of adhesion factors, further mediate the adhesion of leukocytes and monocytes, and aggravate the formation of plaques [29, 30]. Therefore, cell adhesion is also involved in the pathogenesis of AS. Further, PPI analysis showed that forkhead box O 1 (FOXO1), PIK3CA and other proteins were closely related to AS. Some previous studies have also confirmed the role of these proteins in AS. For example, Jian *et al.* found that methyltransferase-like 14 (METTL14) promoted the expression of FOXO1 by enhancing m6a modification, thereby inducing endothelial cell inflammation and plate formation [31].

Here, based on the previous results, we further analyzed the relationship between miR-370-3p and one of its target genes, FOXO1. Validation of dual luciferase reporter genes showed that FOXO1 was indeed a downstream target gene of miR-370-3p, and up-regulation of FOXO1 was observed in both clinical serum samples and ox-LDL-treated VSMCs. FOXO1 was first identified in studies of chromosomal translocations in tumors, and has since been shown to be involved in the progression of various human tumors, such as osteosarcoma [32, 33]. In recent years, new functions of FOXO1 have been gradually revealed. FOXO1 regulates glucose metabolism. In a mouse model, it was found that liver gluconeogenesis was reduced when liver FOXO1 function was deficient, thereby improving fasting blood glucose levels [34]. FOXO1 also regulates lipid metabolism. Overexpression of FOXO1 increased the expression of liver ApoC3 and plasma triglyceride levels [35]. Therefore, the unrestricted expression of FOXO1 in the body can lead to impaired glucose metabolism and lipid metabolism, which is one of the pathogeneses of AS.

The current research has several limitations, which the authors cite as key considerations for future research. In the clinical study, we only analyzed the serum samples of these subjects and did not identify the expression level of SNHG15 in atherosclerotic plaques, so we cannot determine whether the expression of SNHG15 in plate tissue samples is consistent with that in serum. Previous studies have shown that the regulation of AS by non-coding RNA involves many pathways, such as NF-κB, phosphoinositide 3-kinase/protein kinase B (PI3K/AKT) signaling pathway [36, 37]. Whether these pathways are involved in this study remains to be studied. In addition, this study is only the result of cell experiments *in vitro*, and the role of SNHG15/miR-370-3p *in vivo* has not been confirmed. These problems are still the focus of our future research.

In the past few decades, lncRNAs associated with atherosclerotic diseases have only been studied at the tip of the iceberg. Although these studies have indeed found lncRNAs that play an important role in AS, the mechanism through which they affect the occurrence, development, and outcome of AS remains to be further explored. In the future, with the advancement of technology and the deepening of research, lncRNA will gradually play an important role in regulating the pathological process of AS, so as to provide patients with more choices in detection, prevention, intervention and treatment. The highlight of this study is that the clinical samples we included were asymptomatic and non-atherosclerotic people. Therefore, the differentiating value of SNHG15 for these two groups of people may be more meaningful.

In conclusion, the results of this study showed that the expression of SNHG15 increased in AS patients and ox-LDL-induced VSMCs. In addition, SNHG15 may be involved in regulating the proliferation, migration and inflammatory response of VSMCs induced by ox-LDL by down-regulating the expression of miR-370-3p. This new molecular mechanism may provide a new target for the control and treatment of AS.

Acknowledgments

Wan Pan and Yan Zhou contributed equally to the text.

Funding

No external funding.

Ethical approval

This study was approved by the Ethics Committee of Wuhan No. 1 Hospital (No. 2020 number 6).

Conflict of interest

The authors declare no conflict of interest.

References

1. Hansson GK, Hermansson A. The immune system in atherosclerosis. Nat Immunol 2011; 12: 204-12.
2. Falk E. Pathogenesis of atherosclerosis. J Am Coll Cardiol 2006; 47 (8 Suppl): C7-12.
3. Fan J, Watanabe T. Atherosclerosis: known and unknown. Pathol Int 2022; 72: 151-60.
4. Bennett MR, Sinha S, Owens GK. Vascular smooth muscle cells in atherosclerosis. Circ Res 2016; 118: 692-702.
5. Grootaert MOJ, Moulis M, Roth L, et al. Vascular smooth muscle cell death, autophagy and senescence in atherosclerosis. Cardiovasc Res 2018; 114: 622-34.
6. Pedro-Botet J, Climent E, Benaiges, D. Atherosclerosis and inflammation. New therapeutic approaches. Med Clin (Barc) 2020; 155: 256-62.
7. Hu YW, Guo FX, Xu YJ, et al. Long noncoding RNA NEXN-AS1 mitigates atherosclerosis by regulating the actin-binding protein NEXN. J Clin Invest 2019; 129: 1115-28.
8. Ballantyne MD, Pinel K, Dakin R, et al. Smooth muscle enriched long noncoding RNA (SMILR) regulates cell proliferation. Circulation 2016; 133: 2050-65.
9. Shen Y, Liu S, Fan J, et al. Nuclear retention of the lncRNA SNHG1 by doxorubicin attenuates hnRNPC-p53 protein interactions. EMBO Rep 2017; 18: 536-48.
10. Deng QW, Li S, Wang H, et al. Differential long noncoding RNA expressions in peripheral blood mononuclear cells for detection of acute ischemic stroke. Clin Sci (Lond) 2018; 132: 1597-614.
11. Wen Y, Zhang X, Liu X, Huo Y, Gao Y, Yang Y. Suppression of lncRNA SNHG15 protects against cerebral ischemia-reperfusion injury by targeting miR-183-5p/FOXO1 axis. Am J Transl Res 2020; 12: 6250-63.
12. Chen Y, Guo H, Li L, et al. Long non-coding RNA (lncRNA) small nucleolar RNA host gene 15 (SNHG15) alleviates osteoarthritis progression by regulation of extracellular matrix homeostasis. Med Sci Monit 2020; 26: e923868.
13. Kablak-Ziembicka A, Badacz R, Okarski M, Wawak M, Przewlocki T, Podolec J. Cardiac microRNAs: diagnostic and therapeutic potential. Arch Med Sci 2023; 19: 1360-81.
14. Mao J, Wang L, Wu J, et al. miR-370-3p as a novel biomarker promotes breast cancer progression by targeting FBLN5. Stem Cells Int 2021; 2021: 4649890.
15. Wei CY, Zhu MX, Lu NH, et al. Circular RNA circ_0020710 drives tumor progression and immune evasion by regulating the miR-370-3p/CXCL12 axis in melanoma. Mol Cancer 2020; 19: 84.
16. Mao X, Wang L, Chen C, Tao L, Ren S, Zhang L. Circ_0124644 enhances ox-LDL-induced cell damages in human umbilical vein endothelial cells through upregulating FOXO4 by sponging miR-370-3p. Clin Hemorheol Microcirc 2022; 81: 135-47.
17. Authors/Task Force M, Catapano AL, Graham I, et al. 2016 ESC/EAS Guidelines for the Management of Dyslipidaemias: The Task Force for the Management of Dyslipidaemias of the European Society of Cardiology (ESC) and European Atherosclerosis Society (EAS) Developed with the special contribution of the European Association for Cardiovascular Prevention & Rehabilitation (EACPR). Atherosclerosis 2016; 253: 281-344.
18. Chistiakov DA, Melnichenko AA, Myasoedova VA, Grechko AV, Orekhov AN. Mechanisms of foam cell formation in atherosclerosis. J Mol Med (Berl) 2017; 95: 1153-65.
19. Chen D, Zhang M. GAS5 regulates diabetic cardiomyopathy via miR-221-3p/p27 axis-associated autophagy. Mol Med Rep 2021; 23: 135.
20. Lou C, Li T. Long non-coding RNA SENCR alleviates endothelial-to-mesenchymal transition via targeting miR-126a. Arch Med Sci 2023; 19: 180-8.
21. Pi S, Mao L, Chen J, et al. The P2RY12 receptor promotes VSMC-derived foam cell formation by inhibiting autophagy in advanced atherosclerosis. Autophagy 2021; 17: 980-1000.
22. Burger F, Baptista D, Roth A, et al. NLRP3 inflammasome activation controls vascular smooth muscle cells phenotypic switch in atherosclerosis. Int J Mol Sci 2021; 23: 340.
23. Chen Z, Ouyang C, Zhang H, et al. Vascular smooth muscle cell-derived hydrogen sulfide promotes atherosclerotic plaque stability via TFEB (transcription factor EB)-mediated autophagy. Autophagy 2022; 18: 2270-87.
24. Wang Y, Ding M, Yuan X, et al. lncRNA SNHG15 promotes ovarian cancer progression through regulated CDK6 via sponging miR-370-3p. Biomed Res Int 2021; 2021: 9394563.
25. Ding P, Ding Y, Tian Y, Lei X. Circular RNA circ_0010283 regulates the viability and migration of oxidized low-density lipoprotein-induced vascular smooth muscle cells via an miR-370-3p/HMGB1 axis in atherosclerosis. Int J Mol Med 2020; 46: 1399-408.
26. Zhang P, Li X, Zhang S, et al. miR-370-3p regulates adipogenesis through targeting Mknk1. Molecules 2021; 26: 6926.
27. Hildebrandt A, Kirchner B, Meidert AS, et al. Detection of atherosclerosis by small RNA-sequencing analysis of extracellular vesicle enriched serum samples. Front Cell Dev Biol 2021; 9: 729061.
28. Ding Y, Zhou Y, Ling P, et al. Metformin in cardiovascular diabetology: a focused review of its impact on endothelial function. Theranostics 2021; 11: 9376-96.
29. Pacher P, Mechoulam R. Is lipid signaling through cannabinoid 2 receptors part of a protective system? Prog Lipid Res 2011; 50: 193-211.
30. Wu YY, Li XF, Wu S, et al. Role of the S100 protein family in rheumatoid arthritis. Arthritis Res Ther 2022; 24: 35.
31. Jian D, Wang Y, Jian L, et al. METTL14 aggravates endothelial inflammation and atherosclerosis by increasing FOXO1 N6-methyladeosine modifications. Theranostics 2020; 10: 8939-56.
32. Anderson MJ, Viars CS, Czekay S, Cavenee WK, Arden KC. Cloning and characterization of three human forkhead genes that comprise an FKHR-like gene subfamily. Genomics 1998; 47: 187-99.
33. Bai Y, Chen Y, Chen X, et al. Trichostatin A activates FOXO1 and induces autophagy in osteosarcoma. Arch Med Sci 2019; 15: 204-13.
34. Matsumoto M, Pocai A, Rossetti L, Depinho RA, Accili D. Impaired regulation of hepatic glucose production in mice lacking the forkhead transcription factor Foxo1 in liver. Cell Metab 2007; 6: 208-16.
35. Mendivil CO, Zheng C, Furtado J, Lel J, Sacks FM. Metabolism of very-low-density lipoprotein and low-density lipoprotein containing apolipoprotein C-III and not other small apolipoproteins. Arterioscler Thromb Vasc Biol 2010; 30: 239-45.
36. Pan JX. LncRNA H19 promotes atherosclerosis by regulating MAPK and NF-kB signaling pathway. Eur Rev Med Pharmacol Sci 2017; 21: 322-8.
37. Zhao Y, Qian Y, Sun Z, et al. Role of PI3K in the progression and regression of atherosclerosis. Front Pharmacol 2021; 12: 632378.